




Article

The occurrence of wakefieldite, a rare earth element vanadate, in the rhyolitic Joe Lott Tuff, Utah, USA

Bogusław Bagiński^{1*} , Ray Macdonald^{1,2}, Harvey E. Belkin³, Jakub Kotowski¹, Petras Jokubauskas¹ and Beata Marciniak-Maliszewska¹

¹Institute of Geochemistry, Mineralogy and Petrology, University of Warsaw, 02-089 Warsaw Poland; ²Environment Centre, Lancaster University, Lancaster LA1 4YQ, UK; and ³U.S. Geological Survey retired, 11142 Forest Edge Drive, Reston, VA 20190-4026, USA

Abstract

The high-silica rhyolitic Joe Lott Tuff was erupted at 19.2 ± 0.4 Ma from the Mount Belknap caldera, SW Utah. Certain units in the tuff contain two species of wakefieldite, the Nd- and Y-dominant types. They occur in disseminated streaks and patches in association with rhodochrosite, calcite, Fe oxide, cerite-(Ce), and a Mn silicate (caryopilite?), thought to have been deposited from hydrothermal fluids. The wakefieldites contain the highest levels of As (≤ 15.34 wt.% As_2O_5) and P (≤ 5.7 wt.% P_2O_5) yet recorded in this mineral, indicating significant solid solution towards chernovite-(Y) and xenotime-(Y). Thorium levels are also unusually high (≤ 14.2 wt.% ThO_2). The source of the hydrothermal fluid(s) is unknown but might be related to uranium mineralisation in the region, in that As, V and U are commonly associated in such deposits.

Keywords: Joe Lott Tuff, wakefieldite-(Nd), wakefieldite-(Y), As, P and Th enrichment

(Received 1 August 2019; accepted 6 October 2019; Accepted Manuscript published online: 14 October 2019; Associate Editor: Anthony R Kampf)

Introduction

Four species of the rare earth element (REE) vanadate wakefieldite, ideally $(\text{REE}, \text{Y})(\text{VO}_4)$, are known: wakefieldite-(Ce) (Deliens and Piret, 1977, 1986), wakefieldite-(La) (Witzke *et al.*, 2008), wakefieldite-(Nd) (Moriyama *et al.*, 2010), and wakefieldite-(Y) (Miles *et al.*, 1971). They occur in a large number of parageneses, including Fe–Mn deposits, granitic pegmatites and silicified wood, and in a wide range of mineral associations. All occurrences of which we are aware, and their host rocks, are listed in the Supplementary Material (see below), although some reports are not accompanied by confirmatory X-ray diffraction or electron microprobe analytical data. Published analyses have shown that there is considerable compositional variation in wakefieldites, with significant degrees of solid solution between each species and with chernovite (YAsO_4) and xenotime (YPO_4). Silicon and Th can also be significant components.

This paper describes previously unrecorded wakefieldite-(Nd) and wakefieldite-(Y) from a high-silica (SiO_2 75–77 wt.%) rhyolitic ash-flow deposit, the Joe Lott Tuff, Utah, USA. These new data have allowed us to comment on compositional variation in the phase and to propose the major substitution schemes. It is suggested that the wakefieldites crystallised from carbonate-rich fluids associated possibly with local vanadium–uranium mineralisation.

The four species of ‘wakefieldite’ belong to the xenotime group of minerals and do not themselves form a group. To stress this point, we refer to the four species in general in the plural as ‘wakefieldites’. Suffixes are used where the species is known.

Joe Lott Tuff

The Joe Lott Tuff Member of the Mount Belknap Volcanics is a rhyolitic ash flow tuff sheet associated with the collapse of the Mount Belknap caldera in west-central Utah (Fig. 1; Cunningham and Steven, 1979; Budding *et al.*, 1987). Erupted at 19.2 ± 0.4 Ma, it has a volume of 150 km^3 . The tuff is a composite sheet, changing laterally from a single cooling unit near source to four distinct cooling units distally (Fig. 2). The Lower Unit is up to 64 m thick and has a basal vitrophyre. Initial collapse of the caldera accompanied eruption of the Lower Unit. The unit is followed upwards by a Middle Unit up to 43 m thick, a 26 m thick Pink Unit, and an Upper Unit 31 m thick. The poorly welded, pumice-rich Pink Unit comprises two ash-flow tuffs (17 m and 9 m thick) separated by a fall layer 0.5 m thick (Fig. 3).

The major variability in the tuff is in the degree of welding and the abundance of phenocrysts. The most densely welded, eutaxitic, rocks are at the base of the Lower Unit (the basal vitrophyre); the degree of welding increases upwards in both the Lower and Middle Units (Budding *et al.*, 1987). With the exception of the basal vitrophyre, the groundmass of all samples is essentially devitrified.

*Author for correspondence: Bogusław Bagiński, Email: B.Baginski@uw.edu.pl

Cite this article: Bagiński B., Macdonald R., Belkin H.E., Kotowski J., Jokubauskas P. and Marciniak-Maliszewska B. (2020) The occurrence of wakefieldite, a rare earth element vanadate, in the rhyolitic Joe Lott Tuff, Utah, USA. *Mineralogical Magazine* 84, 109–116. <https://doi.org/10.1180/mgm.2019.66>

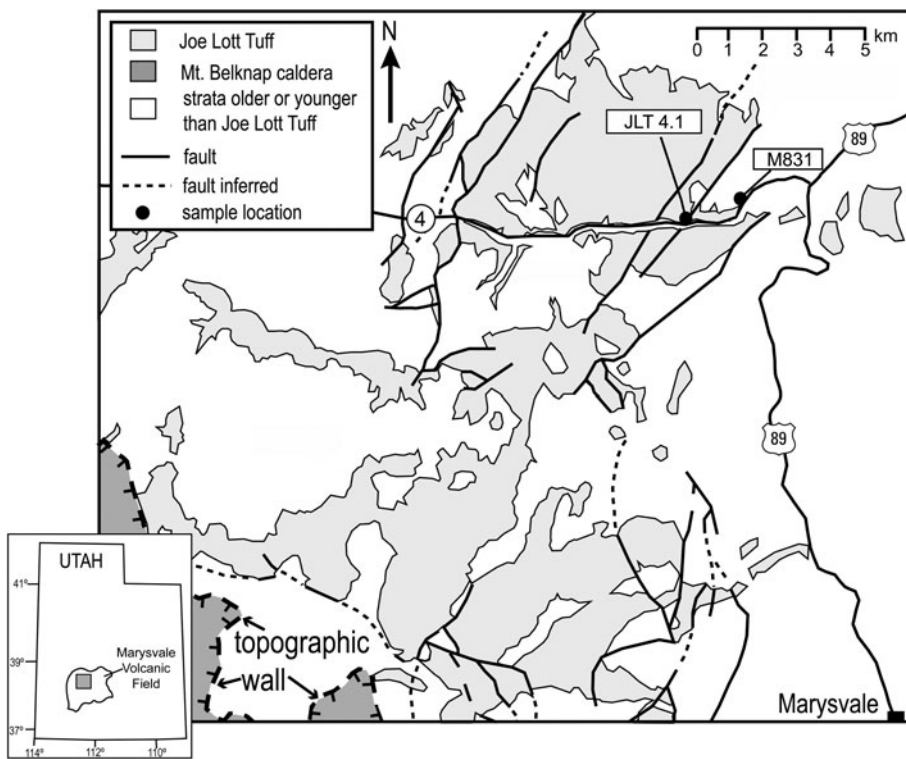


Fig. 1. Locality map of the Mount Belknap Caldera in southwestern Utah, USA, showing the distribution of the Joe Lott Tuff and the location of samples (JLT4.1 and M831) used in this study.

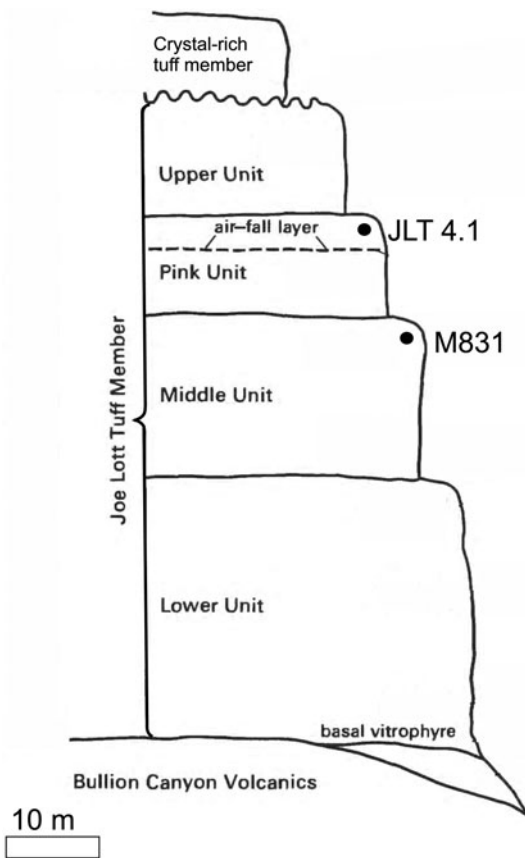


Fig. 2. Stratigraphic relationships in the Joe Lott Tuff Member, the underlying Bullion Canyon Volcanics and the overlying crystal-rich member of the Mount Belknap Volcanics (after Budding *et al.*, 1987, fig. 4). The approximate positions of samples M831 and JLT4.1 are shown.

Occurrence of wakefieldites

Wakefieldites have been investigated in two samples: M831, from the upper part of the Middle Unit; and JLT4.1, from the upper ash-flow layer in the Pink Unit. M831 is poorly welded, with pumices and shards in a devitrified matrix rich in lithophysae up to 0.7 mm across. It contains ~1 modal % phenocrysts of quartz, sanidine, plagioclase, augite, FeTi oxides, apatite, zircon and monazite (Budding *et al.*, 1987). JLT4.1 is more densely welded and lithophysae-bearing, with the principal phenocrysts being alkali feldspar, quartz and magnetite.

The wakefieldites occur in disseminated veins and patches, associated with rhodochrosite, calcite, Fe oxides, cerite-(Ce), a Mn silicate (caryopilite?), monazite and quartz (Fig. 4). The



Fig. 3. Pink Unit, exposed near the junction of State Road 4 and Interstate 89. Two ash-flows are separated by a thin fall layer (white; arrows).

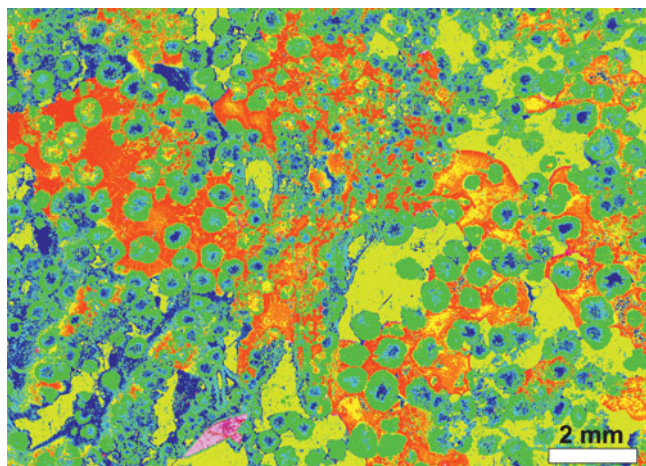


Fig. 4. False colour back-scattered electron (BSE) image of a thin section of JLT4.1. The dark cores of the rounded lithophysae (green) are composed of caryopillite(?) and silica. Yellow areas – calcite; red – rhodochrosite; blue – quartz and alkali feldspar. The pink crystal is magnetite.

assemblage is similar to that of the type wakefieldite-(Nd) from the Arose stratiform deposit, Japan, reported by Moriyama *et al.* (2010) as hematite, caryopillite, calcite and rhodochrosite. In the Joe Lott Tuff, the wakefieldites are relatively abundant: in JLT4.1, over 100 crystals have been identified in a single thin section. Crystals are invariably small; the majority are $\leq 5 \mu\text{m}$ in size, although a few range up to $10 \mu\text{m}$. Representative occurrences of wakefieldite-(Nd) are shown in Fig. 5, in two examples associated with rhodochrosite and two associated with magnetite phenocrysts. The crystals show several habits, including platy, prismatic and rounded. Contacts with neighbouring minerals are normally very well defined.

Analytical methods

Accessory phases were initially identified by scanning electron microscopy (SEM), using a Zeiss SigmaTM/VP FE (field emission) – SEM equipped with new generation SDD-type two Bruker EDS detectors (XFlash 6/10TM). An acceleration voltage of 20 kV was used for the acquisition of the images presented in Figs 4 and 5. Additionally the wakefieldites were analysed with energy dispersive spectroscopy using 5.4 kV, insufficient to excite the V K shell but sufficient to rule out secondary fluorescence effects induced by strong $VK\alpha$ X-rays.

Mineral compositions were determined by electron microprobe analysis, using a Cameca SXFiveFE microprobe equipped with five wavelength-dispersive spectrometers. Four spectrometers were equipped with large diffracting crystals. Wakefieldites were analysed using an electron beam with 15 kV potential and a probe current of 30 nA, reduced to 20 nA for smaller grains. The standards, counting times, diffracting crystals and selected X-ray lines, and approximate detection limits are given in the Appendix. The $\varphi(\rho Z)$ correction model developed by Merlet (1994) was used in the estimates of composition (X-PHI correction model in the *Peaksight* microprobe software).

The preliminary electron microprobe data showed a significant content of Ca (0.53–4.80 wt.% CaO: average 1.20 wt.%). These values are, however, an artefact, caused by secondary fluorescence of Ca in the host rhodochrosite, calcite and

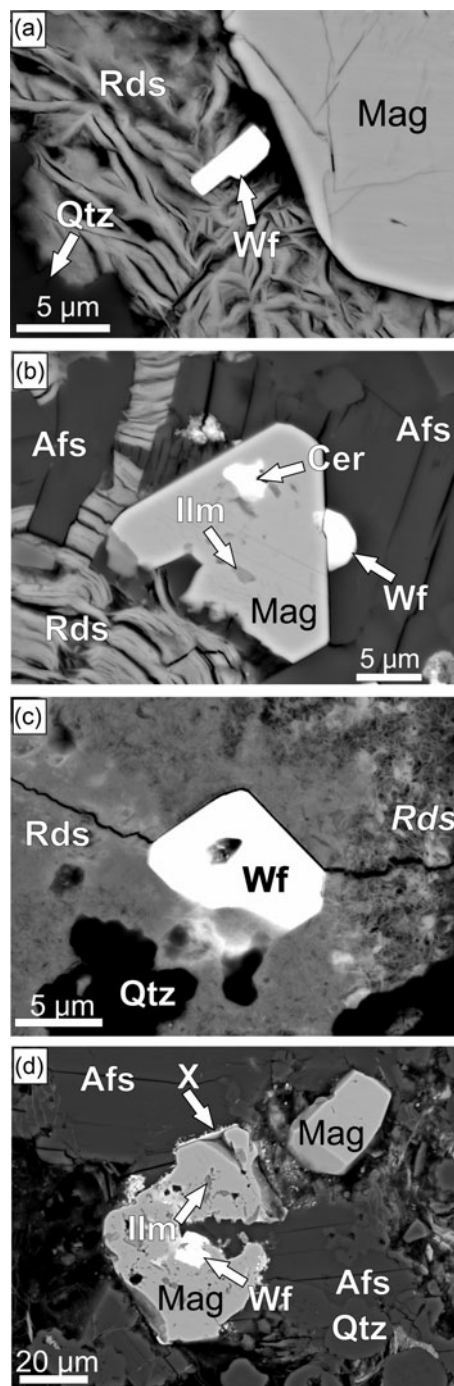


Fig. 5. BSE images of wakefieldite-(Nd) (Wf). (a) In rhodochrosite (Rds) associated with magnetite phenocryst (Mag). (b) Associated with magnetite phenocryst, which also has inclusions of cerite-(Ce) (Cer) and ilmenite (Ilm). Afs is an alkali feldspar phenocryst. (c) Subhedral crystal embedded in rhodochrosite. Rds is italicised to show the textural difference to that in Fig. 5a; the darker Rds to the right is more calcic. Qtz – quartz. (d) As an inclusion in magnetite phenocryst. The pale rim marked X is an unidentified Mn, Pb, Al, Ca silicate.

Ca-bearing glass. To rule out Ca from the wakefieldite structure, a few energy-dispersive spectra were acquired at 15 kV and 5.4 kV acceleration voltages on the same crystal. The significant reduction of $CaK\alpha$ observed with the reduced acceleration voltage and with the absence of $VK\alpha$ x-rays, shows that the wakefieldites studied contain no, or insignificant, amounts of Ca. Accordingly,

Table 1. Representative compositions of wakefieldites in the Joe Lott Tuff.

Sample	Wakefieldite-(Nd)				Wakefieldite-(Y)			
	JLT4.1 1	2	3	4	JLT4.1 5	M831 6	7	8
Wt.%								
P ₂ O ₅	0.72	0.54	0.68	0.62	1.95	5.73	3.15	3.36
V ₂ O ₅	29.38	32.54	31.11	32.78	26.30	13.43	17.26	16.46
As ₂ O ₅	3.13	1.56	2.80	1.45	5.24	12.80	10.58	10.15
Nb ₂ O ₅	bd	0.10	bd	bd	–	–	–	–
SiO ₂	1.40	1.20	1.04	0.88	1.51	3.21	3.00	3.42
TiO ₂	bd	0.12	bd	0.11	bd	–	–	–
ThO ₂	5.62	8.04	6.56	5.61	5.04	11.29	12.89	14.18
UO ₂	bd	bd	bd	bd	bd	bd	bd	bd
SO ₃	bd	bd	bd	bd	bd	0.10	0.05	0.06
Y ₂ O ₃	5.93	5.85	5.59	6.13	13.91	17.11	13.12	12.58
La ₂ O ₃	7.82	10.62	8.74	10.39	4.22	0.47	0.64	0.70
Ce ₂ O ₃	3.60	2.42	2.47	2.23	3.96	3.20	4.14	4.34
Pr ₂ O ₃	5.79	5.66	5.43	6.01	4.16	0.28	0.53	0.50
Nd ₂ O ₃	20.13	19.05	20.27	20.27	14.54	6.82	9.38	8.58
Sm ₂ O ₃	4.63	3.59	4.61	3.87	3.43	3.71	4.46	4.07
Eu ₂ O ₃	0.11	0.19	0.16	0.06	0.14	0.29	0.40	0.36
Gd ₂ O ₃	3.23	2.86	3.38	3.04	3.37	4.67	4.89	4.55
Tb ₂ O ₃	0.39	0.31	0.32	0.31	0.42	0.81	0.82	0.79
Dy ₂ O ₃	3.23	2.97	3.42	2.08	2.97	5.75	5.27	5.00
Ho ₂ O ₃	0.18	0.27	0.30	0.10	0.39	1.01	0.76	0.84
Er ₂ O ₃	0.93	0.87	0.98	0.78	1.40	2.84	2.23	2.31
Tm ₂ O ₃	0.11	0.17	bd	0.13	0.20	0.42	0.34	0.24
Yb ₂ O ₃	0.38	0.29	0.34	0.33	1.26	2.52	1.71	1.69
CaO	1.04	1.28	0.99	1.92	4.80	0.61	0.68	0.84
FeO*	–	–	–	–	–	0.05	0.43	bd
SrO	0.10	bd	bd	0.07	bd	–	–	–
PbO	bd	0.04	bd	bd	0.05	–	–	–
Total	97.85	100.54	99.19	99.17	99.26	97.12	96.73	95.02

Formulae on the basis of 4 oxygens

Ti	0.000	0.004	0.000	0.004	0.000	–	–	–
Th	0.056	0.078	0.064	0.055	0.050	0.110	0.130	0.146
U	0.000	0.000	0.000	0.000	0.000	0.000	0.000	0.000
S	0.000	0.000	0.000	0.000	0.000	0.003	0.002	0.002
Y	0.137	0.130	0.127	0.137	0.304	0.389	0.308	0.300
La	0.127	0.166	0.139	0.164	0.068	0.007	0.010	0.012
Ce	0.058	0.038	0.039	0.035	0.063	0.050	0.067	0.072
Pr	0.092	0.086	0.084	0.092	0.062	0.004	0.009	0.008
Nd	0.316	0.289	0.312	0.311	0.225	0.105	0.149	0.139
Sm	0.070	0.053	0.068	0.057	0.051	0.055	0.068	0.063
Eu	0.002	0.003	0.002	0.001	0.002	0.004	0.006	0.006
Gd	0.047	0.040	0.048	0.043	0.049	0.067	0.072	0.068
Tb	0.006	0.004	0.005	0.004	0.006	0.011	0.012	0.012
Dy	0.046	0.041	0.048	0.029	0.042	0.080	0.075	0.073
Ho	0.003	0.004	0.004	0.001	0.005	0.014	0.011	0.012
Er	0.013	0.012	0.013	0.011	0.019	0.038	0.031	0.033
Tm	0.001	0.002	0.000	0.002	0.003	0.006	0.005	0.003
Yb	0.005	0.004	0.004	0.004	0.017	0.033	0.023	0.023
Fe ²⁺	–	–	–	–	–	0.002	0.016	0.000
Sr	0.003	0.000	0.000	0.002	0.000	0.000	0.000	0.000
Pb	0.000	0.001	0.000	0.000	0.002	–	–	–
Sum	0.979	0.954	0.959	0.952	0.968	0.978	0.995	0.972
P	0.027	0.019	0.025	0.023	0.072	0.208	0.118	0.129
V	0.852	0.913	0.886	0.929	0.754	0.381	0.507	0.492
As	0.072	0.035	0.063	0.033	0.119	0.288	0.246	0.240
Nb	0.000	0.002	0.000	0.000	–	–	–	–
Si	0.061	0.051	0.045	0.038	0.066	0.138	0.133	0.155
Sum	1.012	1.020	1.019	1.022	1.011	1.015	1.004	1.016
Σcations	1.99	1.97	1.98	1.97	1.98	1.99	2.00	1.99

FeO*, all Fe as Fe²⁺. 'bd' = below detection. '–' = not determined.

the CaO data are presented in Table 1 and Table S1 (Supplementary – see below), but Ca is not included in the formula calculations.

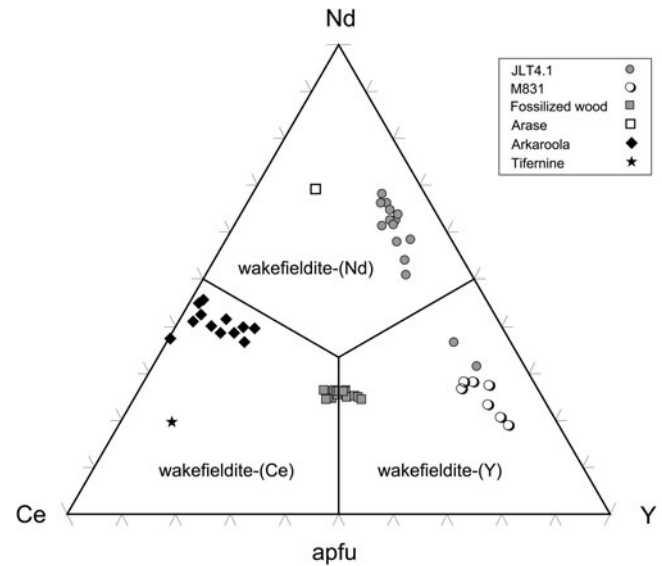


Fig. 6. Ce–Nd–Y (apfu) plot for the Joe Lott Tuff and comparative suites. Data sources: Joe Lott Tuff – Table S1; fossilised wood – Matysová *et al.* (2016); Arase – Moriyama *et al.* (2010); Arkaroola – Bakker and Elburg (2006); Tifernine – Baudracco-Gritti *et al.* (1987). Wakefieldite-(La) is not plotted.

Mineral compositions**Composition of wakefieldite-(Nd) and wakefieldite-(Y)**

Sample JLT4.1 contains both wakefieldite-(Nd) and wakefieldite-(Y); M831 has only wakefieldite-(Y) (Fig. 6; Table 1). After Nd, the most abundant REE in wakefieldite-(Nd) is La, followed by Y. Total REE + Y are in the range 0.82–0.90 apfu. The chondrite-normalised REE patterns (Fig. 7a) show strong negative Ce anomalies ($Ce/Ce^* = 0.08–0.18$), peaks at Pr, then a steady decrease to the HREE (Gd–Yb) with large negative Eu anomalies ($Eu/Eu^* = 0.06–0.30$). The minor troughs at Ho in some patterns may be an artefact as the levels of the element are close to the detection limits. Inter-crystal variations are exemplified by $[La/Ce]_{CN} = 4–12$ and $[La/Yb]_{CN} = 6–24$ (CN – chondrite normalised). The dominant cation replacing the REE is Th (0.05–0.09 apfu). Arsenic (0.03–0.11 apfu) is the main substituent for V (0.77–0.89 apfu), with lesser amounts of P (0.02–0.04 apfu) and Si (≤ 0.04 apfu).

Compared to the Nd-dominant variety, wakefieldite-(Y) in M831 has higher Th (0.05–0.15 apfu), As (0.05–0.37 apfu), P (0.04–0.11 apfu) and Si (≤ 0.20 apfu), and lower REE + Y (0.69–0.75 apfu), and V (0.36–0.76 apfu). The crystals show, with one exception, positive Ce anomalies ($Ce/Ce^* = 1.4–2.2$), a peak at Sm, and have negative Eu anomalies ($Eu/Eu^* = 0.13–0.26$) (Fig. 7b). The wakefieldite-(Y) contains ≤ 0.18 wt.% SO₃ (≤ 0.01 apfu). The only other report of anions in wakefieldite of which we are aware is of SO₃ in fossilised wood from the Czech Republic (0.14 wt.%; Matysová *et al.*, 2016), although Khoury *et al.* (2015) refer to the occurrence in marbles in central Jordan of a Ca- rich, U- and S-bearing analogue of wakefieldite-(Ce) [(Ce,Ca,U)(VO₄)(SO₄)]. The wakefieldite-(Y) from sample JLT4.1 is different to that in sample M831 in having lower abundances of As, P, Th and V (Fig. 8). The patterns in chondrite-normalised REE plots in JLT4.1 are broadly similar to those for wakefieldite-(Nd) in the same rock (Figs. 7a, b).

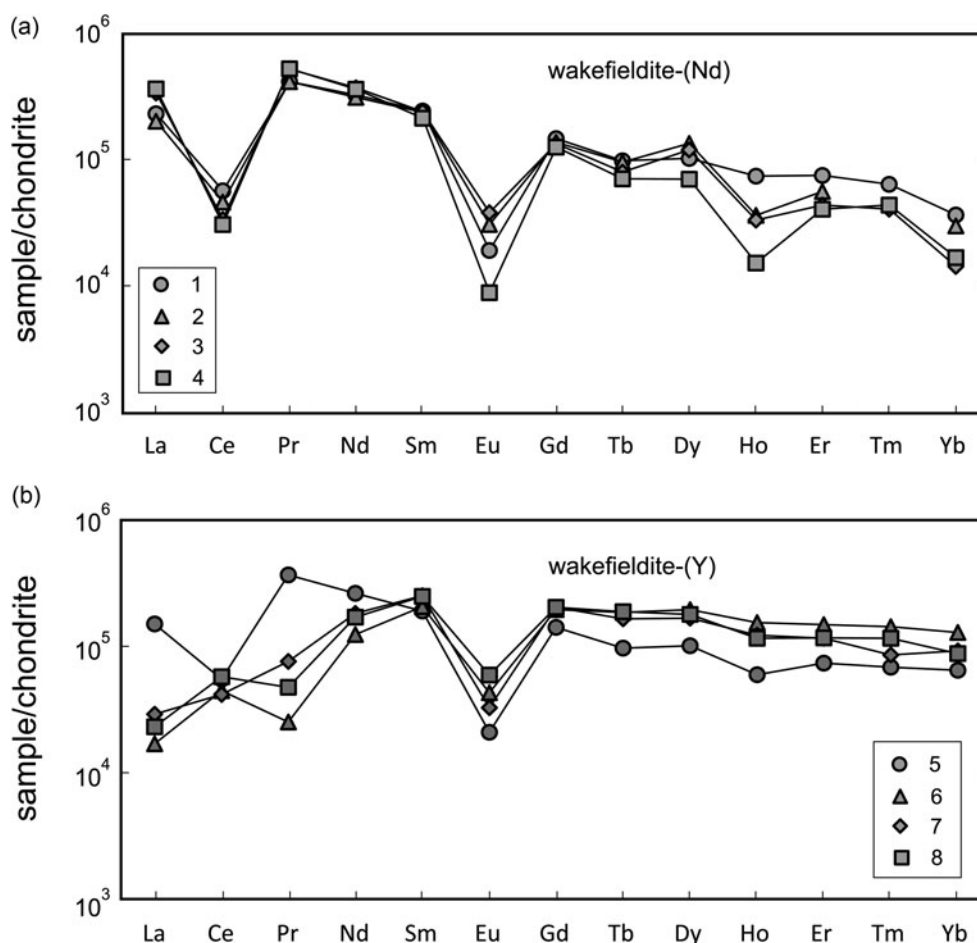


Fig. 7. Chondrite-normalised REE plots for (a) wakefieldite-(Nd) and (b) wakefieldite-(Y) in the Joe Lott Tuff. Data source: Table S1, analysis numbers 1, 4, 9, 13, 14, 16, 22 and 17. Normalising factors from Sun and McDonough (1989).

Substitution mechanisms

In this section, the new and published compositions are used to determine generally applicable substitution schemes. Among the REE, the main substitution is $LREE_1(Y,HREE)_{-1}$, where LREE are La–Eu (Fig. 9).

The major substituent for V in the Joe Lott samples is As (As_1V_{-1}), with As levels up to 0.37 apfu (15.34 wt.% As_2O_5) in wakefieldite-(Y) (Fig. 8a). These are the highest values yet recorded in wakefieldites. In their study of LREE- and Y-arsenates from an Fe–Mn deposit in the Maritime Alps, Miyawaki and Nakai (1996) found up to 30 mol.% of $LREEVO_4$, broadly similar in amount to the entry of As into wakefieldites. Phosphorus also substitutes for V (P_1V_{-1}) in significant amounts in the Joe Lott minerals (≤ 0.11 apfu; 5.7 wt.% P_2O_5), again the highest values yet recorded in wakefieldites (Fig. 8b). It is still uncertain, however, whether there is a complete YVO_4 – YPO_4 solid solution (Kolitsch and Holtstam, 2004; Hetherington *et al.*, 2008). Silicon is present at levels ≤ 0.19 apfu (4.1 wt.% SiO_2), although some high values may be due to beam contamination by neighbouring quartz grains. A positive correlation between Th and Si is here taken to suggest that the Si is incorporated structurally into wakefieldites by the substitution $(REE,Y)^{3+} + V^{5+} \leftrightarrow Th^{4+} + Si^{4+}$, i.e. it is broadly analogous to the huttonite-type substitution in monazite (Fig. 10a).

As noted above, in their study of LREE and Y arsenates Miyawaki and Nakai (1996) found up to 30 mol.% of $LREEVO_4$, in LREE and Y arsenates. They suggested that the presence of large AsO_4 tetrahedra could enable Y arsenates to accept the larger LREE ions. In the Joe Lott case, however, the situation is reversed: the highest As contents are accompanied by higher HREE + Y and lower LREE (Fig. 11a,b).

Formation conditions

The wakefieldite-(Nd) and wakefieldite-(Y) in the Joe Lott Tuff are found in veins and patches associated with rhodochrosite, calcite, cerite-(Ce), monazite, quartz, Fe oxide and caryopilite(?), strongly suggesting that they are of hydrothermal origin. This is consistent with the negative Ce anomalies in wakefieldite-(Nd): the mineral was formed in fluids depleted in Ce by oxidation of Ce^{3+} , with the Ce then entering cerite-(Ce) (c.f. Witzke *et al.*, 2008). We have no independent evidence of the *T/P* conditions under which they crystallised. However, Bakker and Elburg (2006) found that wakefieldite-(Ce) in diopside–titanite veins in Arkaroola, Flinders Range, South Australia, was formed by remobilisation of LREE and Y from titanite and/or the granitic host rock by a hydrothermal fluids of fairly pure H_2O at $T < 200^\circ C$ and $P < 50$ MPa.

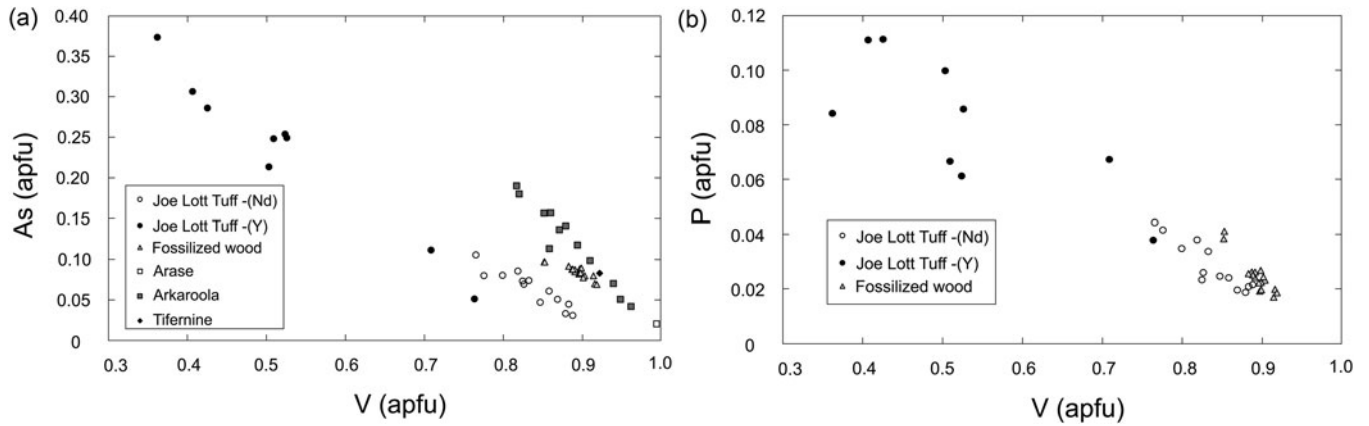


Fig. 8. (a) V vs. As and (b) V vs. P plots for Joe Lott Tuff and comparative suites. Data sources as in Fig. 6.

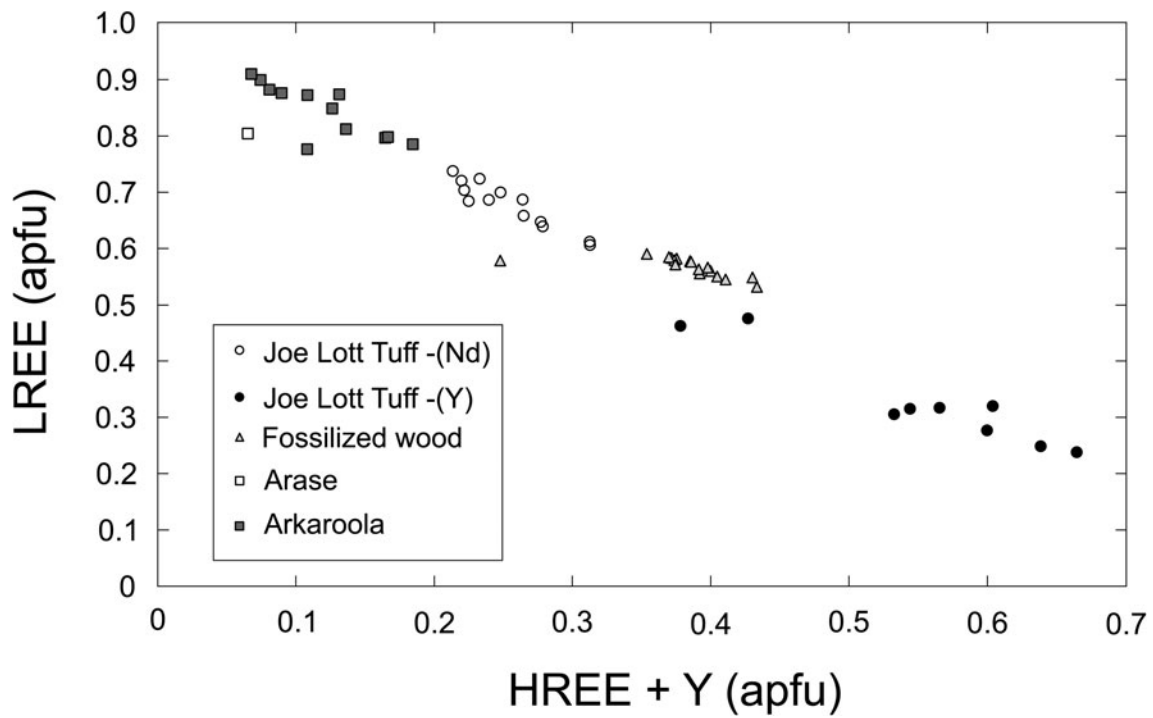


Fig. 9. (Y + HREE) vs. LREE plot for Joe Lott Tuff and comparative suites. Data sources as in Fig. 6, plus Glücksstern-Witzke *et al.* (2008).

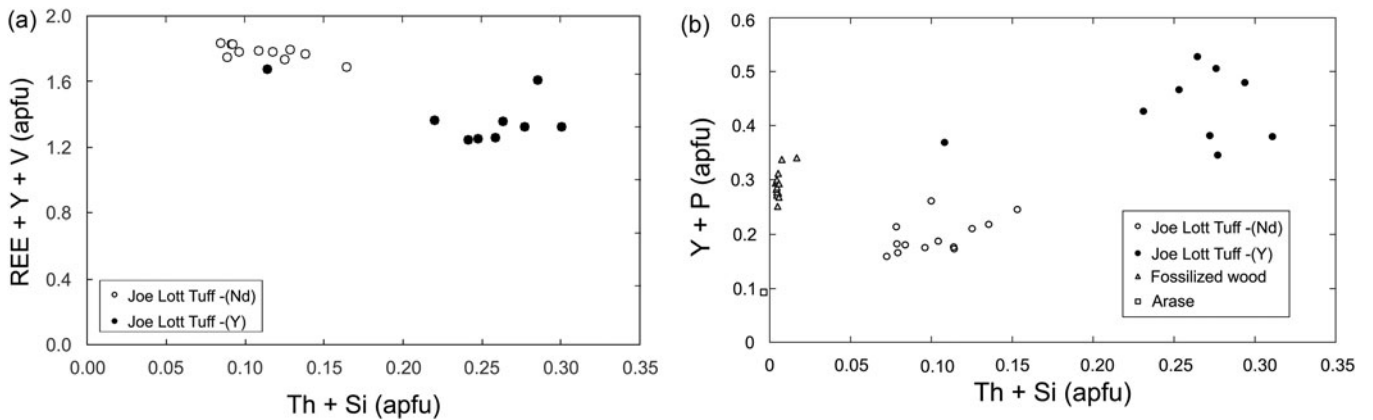


Fig. 10. (a) $(REE, Y)^{3+} + V^{5+} \leftrightarrow Th^{4+} + Si^{4+}$ and (b) $Y^{3+} + P^{5+} = Th^{4+} + Si^{4+}$ as possible substitution schemes in wakefieldites in Joe Lott Tuff.

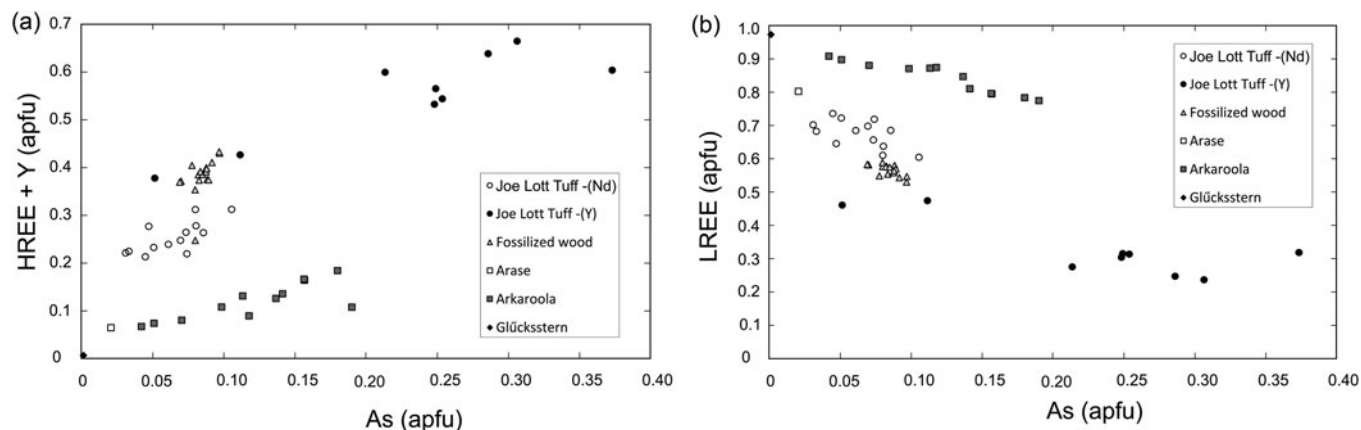


Fig. 11. Arsenic plotted against (a) HREE + Y and (b) LREE for Joe Lott Tuff and comparative suites.

The large number of parageneses in which wakefieldites have been found is reflected in the many mechanisms proposed for their formation. Miles *et al.* (1971) proposed that the type wakefieldite-(Y) is a secondary mineral, possibly derived by leaching of Y-bearing hellandite $[(Ca,REE)_4Y_2Al_2(Si_4B_4O_{22})(OH)_2]$. The type wakefieldite-(Ce) was formed, along with vanadinite $[Pb_5(VO_4)_3Cl]$, in an oxidation zone in a silicified limestone (Deliens and Piret, 1977). Howard *et al.* (1995) reported wakefieldite-(Ce) occurring with Sr-rich zeolites and fluorite, suggesting that the REE and V were carried by hydrothermal solutions during the last stages of formation of the zeolites. Wakefieldite-(Ce) occurs with roscoelite, a vanadium mica, in reduction spots in Devonian sandstones in Banffshire, Scotland. The roscoelite is thought to have formed by a reaction involving a change in redox potential of the groundwater and the release of V from V-rich FeTi oxides in the sandstone (van Panhuys-Sigler *et al.*, 1996). Moriyama *et al.* (2010) proposed that the type wakefieldite-(Nd) was formed during prehnite-pumpellyite facies metamorphism by recrystallisation and hydration of Fe and Mn hydroxide. A solid solution of wakefieldite-(Ce) and wakefieldite-(Y) was formed in silicified plant tissue of Lower Palaeozoic age from the Studenec area, Czech Republic, as a secondary mineral during post-depositional diagenesis (Matysová *et al.*, 2016).

The presence of the oxidised species V^{5+} and As^{5+} and the association of wakefieldites with carbonates in the Joe Lott Tuff strongly suggest that the mineral was deposited from oxidised, pH ≥ 6.5 to 7, CO_2 -rich hydrothermal fluids but this study has provided no evidence of the source of the inferred fluids. However, the Mount Belknap Volcanics (23–14 Ma) formed above a western and eastern source area spanning the central part of the Marysvale volcanic field (Fig. 1). Intrusions in the source area resulted in hydrothermally altered rocks and deposits mostly of uranium and molybdenum (Rowley *et al.*, 1994; Cunningham *et al.*, 1998). The uranium mines in the Marysvale region were operated by the Vanadium Corporation of America. Whereas the mineralisation described in this paper is clearly of a different type, it might also have been related to fluids released by these intrusions.

Supplementary material. To view supplementary material for this article, please visit <https://doi.org/10.1180/mgm.2019.66>.

Acknowledgements. We thank Adam Pieczka and an anonymous reviewer for constructive advice that improved the paper. We also thank Dr Uwe Kolitsch for supplying us with a copy of the 2011 paper by Gröbner *et al.*

on the Harz Mountains occurrence (see Supplementary Material). The work was supported through the Innovative Economy Operational Program POIG.02.02.00-00-025/09 (NanoFun; Cryo-SEM microscopy lab). Financial support was also provided by the project BSt 185704 IGMiP.

References

- Bakker R.J. and Elburg M.A. (2006) A magmatic-hydrothermal transition in Arkaroola (northern Flinders Ranges, South Australia): from diopside-titanite pegmatites to hematite-quartz growth. *Contributions to Mineralogy and Petrology*, **152**, 541–569.
- Baudracco-Gritti C., Quartieri S., Vezzalini G., Permingeat F., Pillard F. and Rinaldi R. (1987) Une wakefieldite-(Ce) non plombifère: nouvelles données sur l'espèce minérale correspondant à l'orthovanadate de cérium. *Bulletin Minéralogique*, **110**, 657–663.
- Budding K.E., Cunningham C.G., Zielinski R.A., Steven T.A. and Stern C.R. (1987) Petrology and chemistry of the Joe Lott Tuff Member of the Mount Belknap Volcanics, Marysvale volcanic field, west-central Utah. *U.S. Geological Survey Professional Paper*, **1354**, 47 pp.
- Cunningham C.G. and Steven T.A. (1979) Mount Belknap and Red Hills calderas and associated rocks, Marysvale volcanic field, west-central Utah. *U.S. Geological Survey Bulletin*, **1468**, 34 pp.
- Cunningham C.G., Rasmussen J.D., Steven T.A., Rye R.O., Rowley P.D., Romberger S.B. and Selverstone J. (1998) Hydrothermal deposits containing molybdenum and fluorite in the Marysvale volcanic field, west-central Utah. *Mineralium Deposita*, **33**(5), 477–494.
- Deliens M. and Piret P. (1977) La kusuïte $(Ce^{3+}, Pb^{2+}, Pb^{4+})VO_4$, nouveau minéral. *Bulletin de la Société Française de Minéralogie et Cristallographie*, **100**, 39–41.
- Deliens M. and Piret P. (1986) La kusuïte devient la wakefieldite-(Ce) plombifère. *Bulletin de Minéralogie*, **109**, 305.
- Hetherington C.J., Jercinovic M.J., Williams M.L. and Mahan K. (2008) Understanding geologic processes with xenotime: Composition, chronology, and a protocol for electron probe microanalysis. *Chemical Geology*, **254**, 133–147.
- Howard D.G., Tschernich R.W. and Klein G.L. (1995) Occurrence of wakefieldite-(Ce) with zeolites at Yellow Lake, British Columbia, Canada. *Neues Jahrbuch für Mineralogie Monatshefte*, **3**, 127–132.
- Khoury H.N., Sokol E.V. and Clark I.D. (2015) Calcium uranium oxide minerals from central Jordan: assemblages, chemistry, and alteration products. *The Canadian Mineralogist*, **53**, 61–82.
- Kolitsch, U. and Holtstam, D. (2004) Crystal chemistry of REEXO₄ compounds (X = P, As, V). II. Review of REEXO₄ compounds and their stability fields. *European Journal of Mineralogy*, **16**, 117–128.
- Matysová P., Götzte J., Leichmann J., Škoda R., Strnad L., Drahotka P. and Grygar T. (2016) Cathodoluminescence and LA-ICP-MS chemistry of silicified wood enclosing wakefieldite – REEs and V migration during complex diagenetic evolution. *European Journal of Mineralogy*, **28**, 869–887.

- Merlet C. (1994) An accurate computer correction program for quantitative electron probe microanalysis. *Microchimica Acta*, **114**, 363–376. <https://doi.org/10.1007/BF01244563>.
- Miles, N.M., Hogarth, D.D. and Russell, D.S. (1971) Wakefieldite, yttrium vanadate: a new mineral from Quebec. *American Mineralogist*, **56**, 395–410.
- Miyawaki R. and Nakai I. (1996) Crystal chemical aspects of rare earth minerals. Pp. 21–40 in: *Rare Earth Minerals. Chemistry, Origin and Ore Deposits* (A.P. Jones, F. Wall and C.T. Williams, editors). Chapman & Hall, London.
- Moriyama T., Miyawaki R., Yokoyama K., Matsubara S., Hirano H., Murakami H. and Watanabe Y. (2010) Wakefieldite-(Nd), a new neodymium vanadate mineral in the Arase stratiform ferromanganese deposit, Kochi Prefecture, Japan. *Resource Geology*, **61**, 101–110.
- Rowley P.D., Mehnert H.H., Naeser C.W., Snee L.W., Cunningham C.G., Steven T.A., Anderson J.J., Sable E.G. and Anderson R.E. (1994) Isotopic ages and stratigraphy of Cenozoic rocks of the Marysvale volcanic field and adjacent areas, west-central Utah. *U.S. Geological Survey Bulletin*, **2071**, 35 pp.
- Sun S.-S. and McDonough W.F. (1989) Chemical and isotopic systematics of oceanic basalts: implications for mantle composition and processes. Pp. 313–345 in: *Magmatism in the Ocean Basins*. (A.D. Saunders and M.J. Norry, editors). Special Publication of the Geological Society, 42. Geological Society, London.
- van Panhuys-Sigler M., Trewin N.H. and Still J. (1996) Roscoelite associated with reduction spots in Devonian red beds, Gamrie Bay, Banffshire. *Scottish Journal of Geology*, **32**, 127–132.
- Witzke T., Kolitsch U., Warnsloh J.M. and Göske J. (2008) Wakefieldite-(La), LaVO₄, a new mineral species from the Glücksstern Mine, Friedrichroda, Thuringia, Germany. *European Journal of Mineralogy*, **20**, 1135–1139.

Appendix. Analytical conditions for the electron microprobe analysis.

Element/ X-ray line	Crystal	Peak overlap corr.	Standard	Approx. det. limit (ppm)	Peak/ backgr. (s)	Approx. S.D. (wt.%)	Element/ X-ray line	Crystal	Peak overlap corr.	Standard	Approx. det. limit (ppm)	Peak/ backgr. (s)	Approx. S.D. (wt.%)
As L α	TAP		ZnAs ₂	760	30/30	0.10	Pr L α	LPET	LaL β , VK α	PrPO ₄	290	30/60	0.06
Ca K α	LPET		Wollast.	160	20/20	0.02	S K α	LPET		FeS ₂	180	20/20	0.01
Ce L α	LPET		CePO ₄	500	30/30	0.06	Si K α	TAP		SiO ₂	220	20/20	0.03
Dy L α	LLIF		DyPO ₄	1460	20/40	0.19	Sm L α	LLIF	CeL β ₂	SmPO ₄	1260	20/40	0.18
Er L α	LLIF	TbL β ₄	ErPO ₄	1450	20/40	0.14	Sr L α	TAP		SrSO ₄	460	30/60	0.04
Eu L α	LLIF	PrL β ₂ , NdL β ₃	EuPO ₄	120	30/60	0.01	Tb L α	LLIF		TbPO ₄	1150	30/60	0.10
Gd L α	LLIF	LaL γ ₂ , CeL γ	GdPO ₄	1280	20/40	0.15	Th M α	LPET		ThO ₂	480	60/120	0.12
Ho L α	LLIF	GdL β	HoPO ₄	160	30/60	0.02	Ti K α	LLIF		TiO ₂	420	20/40	0.03
La L α	LPET		LaPO ₄	470	30/30	0.01	Tm L α	LLIF	SmL γ , DyL β ₄	TmPO ₄	270	30/60	0.02
Nb L α	LPET		Nb (met.)	420	60/60	0.04	U M α	LPET	ThM β	UO ₂	400	80/80	0.02
Nd L α	LLIF	CeL β	NdPO ₄	1200	20/40	0.40	V K α	LLIF		V (met.)	500	20/40	0.31
P K α	TAP	YL β	CePO ₄	260	20/20	0.04	Y L α	TAP		YPO ₄	450	60/60	0.09
Pb M α	LPET	YL γ ₃	Crocoite	200	140/280	0.01	Yb M α	LTAP	DyM γ	YbPO ₄	400	120/120	0.03

Notes: 'peak overlap corr.' – peak overlap correction; 'Approx det limit' – approximate detection limit; 'Peak/backgr.' count time on peak and backgrounds; 'Approx. S.D.' – approximate standard deviation; 'met.' – metal.